

Appropriate solid-body models as initial conditions for SPH-based numerical collision experiments

C. Burger¹, T. I. Maindl¹, R. Dvorak¹, C. Schäfer² and R. Speith³

¹Department of Astrophysics, University of Vienna, Austria

²Institut für Astronomie und Astrophysik, Eberhard Karls Universität Tübingen, Germany

³Physikalisches Institut, Eberhard Karls Universität Tübingen, Germany

Context

(Giant) collisions are an ubiquitous process during all stages of planet formation. To answer questions concerning the transport of volatiles (water), realistic fragmentation behavior, or the formation of the Moon in detail, individual collisions have to be investigated, often by means of SPH simulations (e.g. Maindl et al. 2014).

While planetesimal-scale collisions can be modeled by simple homogeneous bodies, this does not hold for giant collisions anymore, where the bodies' internal (radial) structures generally affect results. In practise some dynamical settling (*numerical relaxation*) is applied in most cases, either starting from some predetermined radial profile or from scratch. Since this procedure has to be carried out prior to the actual simulation run, it requires potentially high computational resources solely for producing the initial conditions.

Semi-analytical relaxation: Self-consistent hydrostatic structures as initial conditions

- Self-consistent (in terms of the applied physical model) hydrostatic profiles are calculated and assigned to the SPH particles (Fig. 3).
- Even though the resulting initial conditions are not entirely equilibrated (see Fig. 1), tests based on several astrophysical criteria with typical giant collision simulations show equal results when compared to fully (numerically) relaxed runs of identical scenarios – this is shown for the evolution of fragment masses and their water-ice content in Fig. 4 for a scenario similar to those in Fig. 2.
- The method's computational costs are very close to zero.

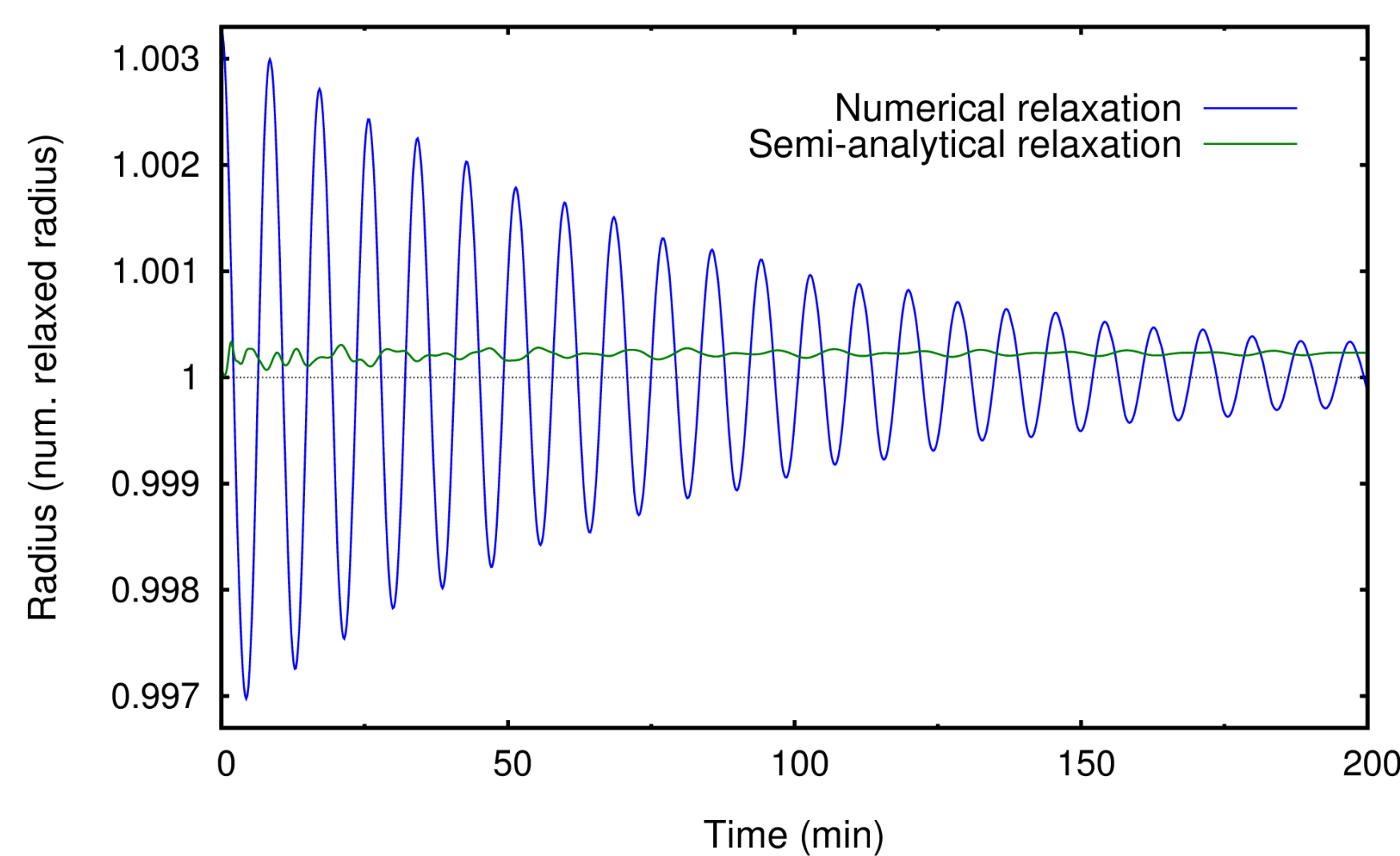
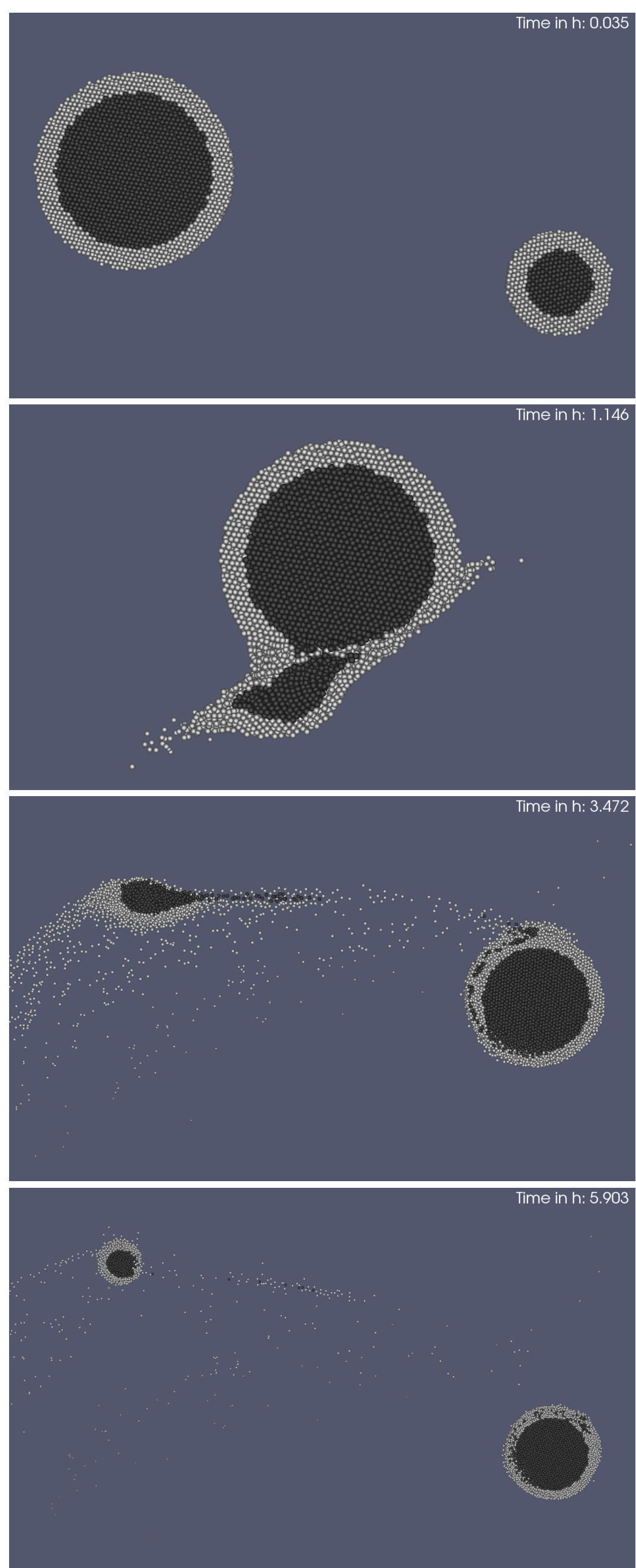


Fig. 1. Comparison of the radial oscillation patterns during numerical relaxation (blue) and after semi-analytical relaxation (green) for a body with $\sim 10 \times M_{\text{Ceres}}$.

General importance of relaxation

- What are the effects of not applying any relaxation at all (i.e. to start with homogeneous bodies) compared to initially relaxed runs for exactly the same scenario (Fig. 2)?
- Typical differences for two out of several considered criteria – fragment masses overall and their water-ice content – are clearly visible in Fig. 4. For the largest and second-largest fragments differences up to a few percent are common between relaxed and unrelaxed runs. By far the greatest differences are found for the rest of the material, where up to 50% more is lost as debris for initially unrelaxed cases.
- Preliminary results show no strong correlation between relaxation relevance and the masses of the colliding bodies (for masses ranging from below Ceres' to above the Moon's).

(Lagrangian) set of equations determining the structure (radius r , pressure p , density ρ and internal energy e) of a hydrostatic sphere, consistent with the simulations' physical model – provided that the same equation of state is used.

$$\frac{dr(m)}{dm} = \frac{1}{4\pi r(m)^2 \rho(m)} \quad \frac{dp(m)}{dm} = -\frac{Gm}{4\pi r(m)^4}$$

$$p = p(\rho, e) \rightarrow \rho = \rho(p, e) = \rho(p, e(\rho)) \rightarrow \rho^{(n+1)} = \rho(p, e(\rho^{(n)}))$$

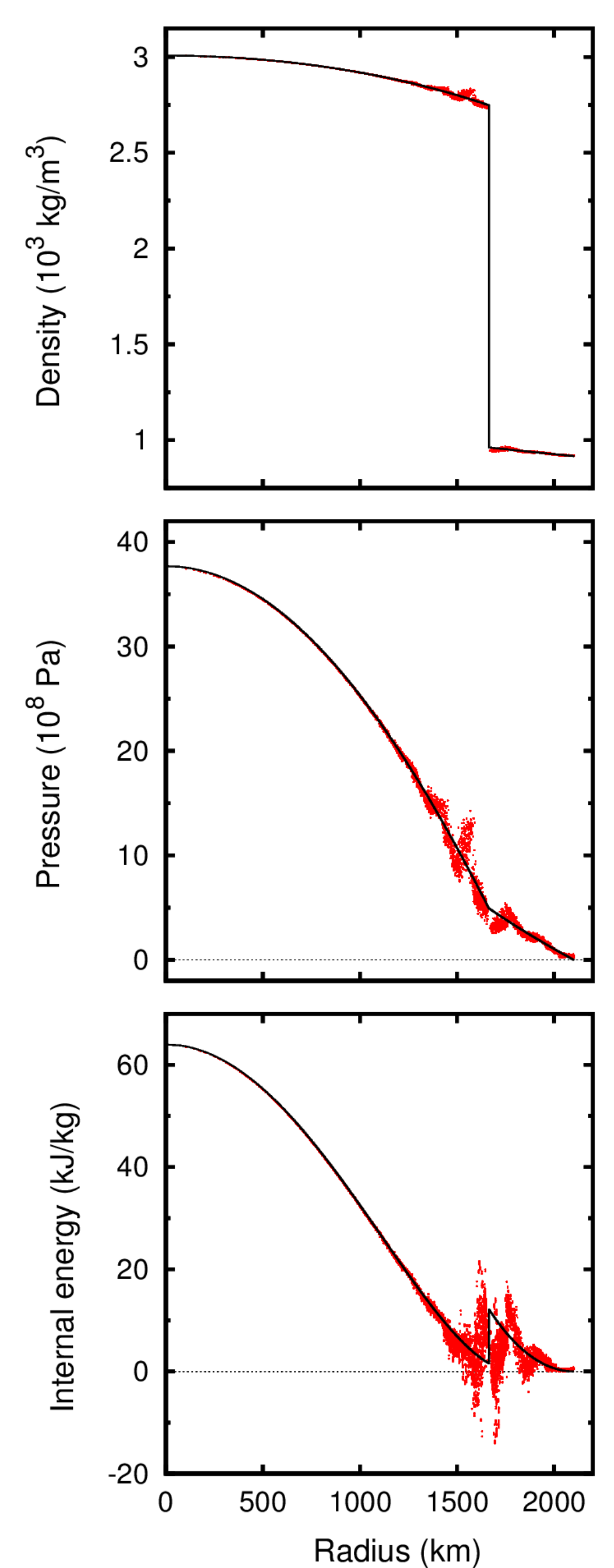


Fig. 3. Comparison of calculated hydrostatic profiles (black) and their appearance after additional numerical relaxation due to remaining fluctuations (see Fig. 1) for a body of $\sim M_{\text{Moon}}$ with a core-shell structure of basalt and water-ice.

profiles (black) and their appearance after additional numerical relaxation due to remaining fluctuations (see Fig. 1) for a body of $\sim M_{\text{Moon}}$ with a core-shell structure of basalt and water-ice.

Fig. 2. Simulation snapshots (cuts) showing the material distribution of basalt (black) and water-ice (white). A $\sim M_{\text{Ceres}}$ projectile is hitting a target about 10 times as massive with a typical velocity of $\sim 1.6 v_{\text{esc}}$ (Maindl and Dvorak 2013). The scenario is similar to the one examined in Fig. 4.

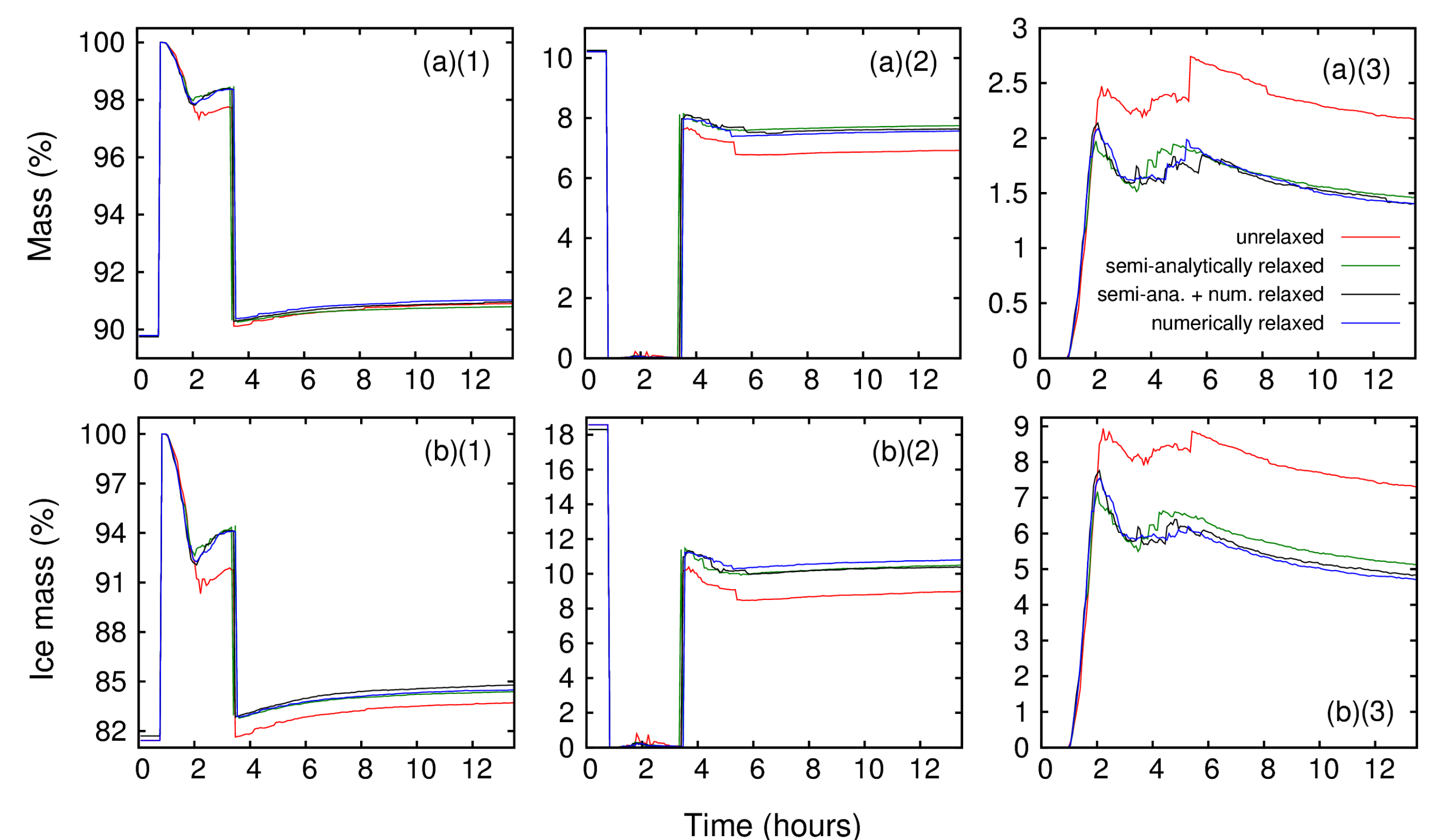


Fig. 4. Evolution of overall fragment masses (a) and water-ice masses (b) (in % of system's total ice mass), for the largest fragment (1), the second-largest fragment (2) and the rest of the material (3). The scenario is similar to Fig. 2. Three different relaxation approaches are plotted along with an initially unrelaxed run (see key), where the semi-analytical method performs similar to the others while the unrelaxed run differs significantly (see text).

Acknowledgements: CB, TIM and RD acknowledge funding by the FWF Austrian Science Fund project S 11603-N16.

References: Maindl, T. I., Dvorak, R., 2013, IAUS, 299, 370. – Maindl, T. I., Dvorak, R., Schäfer, C., Speith, R., 2014, IAUS, 310, 138.